*International Immunology, Vol. 16, No. 7, pp. 915–928*
doi: 10.1093/intimm/dxh093 Advance Access publication May 24, 2004


# Evidence for recruitment of plasmacytoid dendritic cell precursors to inflamed lymph nodes through high endothelial venules

**Hiroyuki Yoneyama, Kenjiro Matsuno[1], Yanyun Zhang, Tetsu Nishiwaki, Masahiro Kitabatake, Satoshi Ueha, Shosaku Narumi, Shunichi Morikawa[2], Taichi Ezaki[2], Bao Lu[3], Craig Gerard[3], Sho Ishikawa** and **Kouji Matsushima**

Department of Molecular Preventive Medicine & SORST, Graduate School of Medicine, University of Tokyo, Bunkyo-ku, Tokyo 113-0033, Japan
[1]Department of Anatomy (Macro) & SORST, Dokkyo University School of Medicine, Tochigi 321-0293, Japan
[2]Department of Anatomy & Developmental Biology, Tokyo Women's Medical University School of Medicine, Tokyo 162-8666, Japan
[3]Department of Pediatrics, Children's Hospital, Harvard Medical School, 300 Longwood Avenue, Boston, Massachusetts 02115, USA

*Key words*: binding, chemokine, migration, selectin, TNF

**Abstract**

**Recruitment of dendritic cells (DCs) to lymph nodes (LNs) is pivotal to the establishment of immune response. Whereas DCs have been proven to undergo afferent lymphatic pathway to enter LNs from peripheral tissues, a question remains if DCs also migrate into LNs directly from the circulation. Here we demonstrate that plasmacytoid DC (pDC) precursors can transmigrate across high endothelial venules (HEVs) of inflamed LNs in mice. Bacterial infection induces a significant number of pDC and myeloid DC (mDC) precursors into the circulation. Both subsets express a common set of chemokine receptors except CXCR3, display parallel mobilization into the blood, but show distinct trafficking pathway to the LNs. In a short-term homing assay, whereas mDC precursors migrate to peripheral tissues and subsequently to draining LNs, pDC precursors directly enter the LNs in a CXCL9 and E-selectin dependent manner. Tumor necrosis factor-α controls not only DC precursor mobilization into the blood but also chemokine up-regulation on LN HEVs. A similar trafficking pathway is observed also in viral infection, and CXCR3$^{-/-}$ mice-derived pDC precursors show defective trans-HEV migration. This study clarifies the inflammation-dependent, chemokine-driven distinct property of DC precursor trafficking.**

## Introduction

DCs determine the type of immune response or tolerance after migrating to LNs (1). Experimentally, neither immature nor mature DCs of myeloid origin have been shown to enter LNs directly from the circulation through high endothelial venules (HEVs) (2,3). They gain access to peripheral tissues instead, whilst antigen-loaded mature DCs migrate into the draining LNs via afferent lymphatics to become interdigitating DCs (IDCs) that promote immunity or maintain tolerance (1). Thus, trafficking of myeloid DCs (mDCs) is quite distinct from that of naive T lymphocytes, which continually circulate from blood to LNs via HEVs (4). These circulatory patterns are effective in establishing immune responses, inasmuch as naive DCs encounter and ingest antigens initially in the peripheral tissues, whereas naive lymphocytes are exposed to antigens presented by IDCs in the LNs, leading to their proliferation and differentiation into appropriate memory T cells. Thus, tissue-experienced mDCs link innate immunity at sites of inflammation with acquired immunity (1,5).

We previously described that chemokines regulate DC trafficking, thereby contributing to the outcome of immune responses (6,7). Intravenously administered *Propionibacterium acnes*, a probable etiologic agent of sarcoidosis (8) which can induce systemic inflammation (9,10), dramatically increased the number of MHCII$^{-}$F4/80$^{-}$B220$^{-}$CD11c$^{+}$ mDC

*Correspondence to*: K. Matsushima; E-mail: koujim@m.u-tokyo.ac.jp

*Transmitting editor*: M. Miyasaka

*Received* 2 March 2004, *accepted* 12 April 2004

precursors in the circulation (6). The direct recruitment of these cells to inflamed liver from the circulation is mediated by the interactions of MIP1-α/CCL3-CCR1 and CCR5. After contributing to the development of inflammatory foci (granulomas) as well as *de novo* peripheral lymphoid tissues (portal tract-associated lymphoid tissue; PALT), the maturing mDCs are remobilized into draining hepatic LNs (HLNs) via afferent lymphatics, in response to SLC/CCL21-CCR7 interactions. Here they contribute to the generation of TH 1 lymphocytes through the interaction of mDC-derived IP-10/CXCL10 with CXCR3 on TH 1 cells (7,11).

In contrast, plasmacytoid DCs (pDCs) and some precursor populations of DCs have been postulated, though not yet proven, to enter the LNs via HEVs in an L-selectin-dependent manner (12,13). However, LN entry via afferent lymphatics from peripheral tissues, but not via HEVs from the blood, is of significance for DCs, because these cells induce peripheral tolerance to self-components of peripheral tissues after migrating to the LNs (14–16). The direct access of blood DCs to secondary LNs without scanning of peripheral tissues may risk circumventing both the DC-mediated linkage of innate and acquired immunity and tolerance. A pivotal question has therefore arisen as to whether DCs can directly transmigrate across HEVs from the circulation like lymphocytes. To know the answer, we have studied homing-associated molecules and the way of LN entry by pDC precursors using HEV-binding and adoptive transfer experiments.

## Methods

### *Mice*

Specific pathogen-free female C57BL/6 mice (8–9 wk old) were obtained from CLEA Japan Inc (Tokyo, Japan). CXCR3 gene deficient mice were generated as reported (17) and back-crossed into C57BL/6 mice for eight generations under specific pathogen-free conditions. All animal experiments complied with the standards set out in the guidelines of the Graduate School of Medicine, University of Tokyo.

### *P. acnes and HSV infection*

For *P. acnes* infection, mice were injected with heat-killed *P. acnes* (ATCC 11828; 1 mg/100 μl PBS) via the tail vein (6). For herpes simplex virus (HSV) infection, the KOS strain of HSV-1 was propagated and titered using VERO cells grown in MEM plus 10% FCS. Mice were infected in the right hind footpad with $5 \times 10^4$ PFU of HSV-KOS, and the popliteal, inguinal and axillary LNs, as well as spleen, skin and peripheral blood, were examined at the times described. Serum tumor necrosis factor (TNF)-α was assayed by ELISA (Endogen, Rockford, IL) (18).

### *FACS, isolation and cell culture of DCs*

Blood MHCII$^-$CD11c$^+$ DC precursors were isolated using an EPICS ELITE ESP cell sorter (Beckman Coulter, Hialeah, FL) or a MACS system (Miltenyi Biotech, Bergisch Gladbach, Germany) as described (6). For cell sorting, MHCII$^-$, CD19$^-$, CD3$^-$ and DX5-depleted blood cells were stained with anti-CD11c–FITC mAb and anti-B220–PE mAb (BD Pharmingen, San Diego, CA). Analysis of the sorted population showed purity >99%. For cell phenotyping, blood mononuclear cells were stained with various biotinylated mAbs against homing molecules and Cy-chrome-conjugated streptavidin, followed by incubation with PE-labeled anti-B220 and FITC-labeled anti-CD11c mAbs.

Purified B220$^+$ and B220$^-$CD11c$^+$ cells ($1 \times 10^5$ cells/200 μl well) were incubated for 24 h in round-bottomed 96-well culture plates in RPMI 1640 supplemented with 20% FCS, penicillin G (100 U/ml), and streptomycin (100 μ/ml), in the presence of CpG-ODN 1668 (TCCATGACGTTCCGATGCT; 1 μM) or irradiated HSV (30 PFU/well). IFN-α in the culture supernatants was assayed by ELISA (PBL-Biomedical, Piscataway, NJ). To obtain mature mDCs (Figs 2D, 3B and C), purified B220$^-$CD11c$^+$ cells were incubated with GM-CSF (4 ng/ml, Genzyme-Teche, Cambridge, MA) and TNF-α (50 ng/ml, R&D Systems, Minneapolis, MN) on type I collagen-coated plates (IWAKI, Tokyo, Japan) for 3 days (6). The one-way mixed leukocyte reaction (MLR) was performed in 96-well plates using the premix Water-Soluble Tetrazolium salt (WST)-1 cell proliferation assay system (Takara Biomedicals, Tokyo, Japan) as previously reported (6,19). For *in vivo* phagocytosis, cytosmear preparations of freshly isolated DC precursors were stained for rabbit pAb to *P. acnes* (provided by Dr Y. Eishi; Tokyo Medical and Dental College).

### *Antibodies and immunohistochemistry*

Double immunohistochemical staining was performed as reported (6,7). All PNAd$^+$ HEVs from 10 LNs were counted and scored for the presence of CD11c$^+$ cells. The percentage of DC-positive HEVs (Fig. 10 B) was calculated as 100× the number of PNAd$^+$ HEVs associated with CD11c$^+$ cells, divided by the total number of PNAd$^+$ HEVs.

The following anti-mouse mAbs were used: CD3ε (clone; 145-2C11), CD4 (RM4-5), CD8α (53-6.7), CD11b (M1/70), CD11c (HL3), CD19 (1D3), β1-integrin (Ha2/5), CD45R/B220 (RA3-6B2), α4-integrin (9C10), αV-integrin (RMV-7), CD62L (Mel-14), CD62P (RB40.34), αE-integrin (2E7), β7-integrin (M293), Gr-1 (RB6-8C5), Pan-NK cell (DX5), PNAd carbohydrate epitope (MECA-79), VCAM-1 (429), CXCL12 (12G5) from Pharmingen; F4/80 (CI:A3-1), DEC-205 (NLDC-145), MHC II (ER-TR3) from BMA Biomedicals (Rheinstrasse, Switzerland) and CD11c (N418) from Serotec (Oxford, UK). Goat pAbs to the CCL3 (6) and CXCL9 (7) were purchased from R&D Systems, while those to CXCL10 (7) were from Santa Cruz Biotechnology Inc. (Santa Cruz, CA). Rabbit pAbs to CCL21 (6) and TNF-α (9), and mAbs to CXCL10 (7) and E-selectin (20) were made in house. For control Abs, we used goat IgG, rabbit IgG (Sigma-Aldrich, St. Louis, MO), and anti-human parathyroid-related peptide mAb, which was the IgG1 subclass-matched control mAb (6,7,20,21). For blocking experiments, 100 μg of mAbs, pAbs and a mixture of control Abs were singly injected i.v. just prior to *P. acnes*-treatment (Fig. 4), HSV-treatment (Fig. 9B), or cell transfer.

### *Real-time quantitative RT–PCR*

Total RNA was isolated from $2 \times 10^5$ sorted blood and LN cells using RNAzol$^B$ (BIOTECX Laboratories, Houston, TX) and reverse transcribed. The resultant cDNA was amplified using the ABI 7700 sequence detector system (PE Applied Biosystems, Foster City, CA) with a set of primers and probes

corresponding to chemokine receptors and, as controls, HPRT and GAPDH (6). The sense primer for CCR1 was 5′-GTGTTCATCATTGGAGTGGTGG-3′, the antisense primer was 5′-GGTTGAACAGGTAGATGCTGGTC-3′, the probe was 5′-TGGTGCTCATGCAGCATAGGAGGCTT-3′. The sense primer for CCR2 was 5′-TGTTTACCTCAGTTCATCCACGG-3′, the antisense primer was 5′-CAGAATGGTAATGTGAGC-AGGAAG-3′, the probe was 5′-TCTGCTCAACTTGGCCA-TCTCTGACC-3′. The sense primer for CCR3 was 5′-TTGCAGGACTGGCAGCATT-3′, the antisense primer was 5′-CCATAACGAGGAGAGGAAGAGCTA-3′, the probe was 5′-TGCAGTCCTCGCTATCCAGAAGGTGA-3′. The sense primer for CCR4 was 5′-TCTACAGCGGCATCTTCTTCAT-3′, the antisense primer was 5′-CAGTACGTGTGGTTGTGCTCTG-3′, the probe was 5′-TGATCACGTGGTCAGTGGCTGTGTT-3′. The sense primer for CCR5 was 5′-CATCGATTATGGTATGT-CAGCACC-3′, the antisense primer was 5′-CAGAATGG-TAGTGTGAGCAGGAA-3′, the probe was 5′-TACCTGCTC-AACCTGGCCATCTCTGA-3′. The sense primer for CCR6 was 5′-ACTCTTTGTCCTCACCCTACCG-3′, the antisense primer was 5′-ATCCTGCAGCTCGTATTTCTTG-3′, the probe was 5′-ACGCTCCAGAACACTGACGCACAGTA-3′. The sense primer for CCR7 was 5′-CATCAGCATTGACCGCTACGT-3′, the antisense primer was 5′-GGTACGGATGATAATGAGGTAGCA-3′, the probe was 5′-ATCACCATCCAAGTGGCCCAGATGGT-3′. The sense primer for CCR8 was 5′-ACGTCACGATGACC-GACTACTAC-3′, the antisense primer was 5′-GAGACCACCT-TACACATCGCAG-3′, the probe was 5′-AGATATCTA-CCTCCTGAACCTGGCCGCAT-3′. The sense primer for CCR9 was 5′-CCATTCTTGTAGTGCAGGCTGTT-3′, the antisense primer was 5′-AAGCTTCAAGCTACCCTCTCTCC-3′, the probe was 5′-AGCCTTATGCCATGTTCATCTCCAA-3′. The sense primer for CXCR2 was 5′-CATCTTATACAACCG-GAGCACC-3′, the antisense primer was 5′-TAGTAACCA-CATGGCTATGCACAC-3′, the probe was 5′-CTCTGTCAC-CGATGTCTACCTGCTGAACCT-3′. The sense primer for CXCR3 was 5′-ATCAGCGCTTCAATGCCAC-3′, the sense primer was 5′-TGGCTTTCTCGACCACAGTT-3′, the probe was 5′-ATGCCCATATCCTAGCTGTTCTGCTGGTC-3′. The sense primer for CXCR4 was 5′-CTGAGAAGCATGACGGA-CAAGT-3′, the antisense primer was 5′-TGAGGACACTGCTG-TAGAGGTTG-3′, the probe was 5′-CTTCCTATGCAAGGC-AGTCCATGTCA-3′. The sense primer for CXCR5 was 5′-TCCTACTACCGATGCTTGTGATG-3′, the antisense primer was 5′-ACGCCAGCGAAGGTGTAAA-3′, the probe was 5′-TGTGGCCATCACCTTGTGTGAATTCC-3′. The sense primer for HPRT was 5′-GGCAGTATAATCCAAAGATGGTCAA-3′, the antisense primer was 5′-GTCTGGCTTATATCCAACACTT-CGT-3′, the probe was 5′-CAAGCTTGCTGGTGAAAAG-GACCCC-3′. The sense primer for GAPDH was 5′-AGTATGACTCCACTCACGGCAA-3′, the antisense primer was 5′-TCTCGCTCCTGGAAGATGGT-3′, the probe was 5′-AACGGCACAGTCAAGGCCGAGAAT-3′. The quantity of specific cDNA in each sample was normalized to the quantity of GAPDH cDNA in that sample, and all quantitative values were expressed relative to the normalized amount for HPRT.

### *Chemotaxis assay*

DC precursors before and after culture ($5 \times 10^5$ cells/100 μl) were loaded into murine type IV collagen-coated transwells (3 μm pore size, Becton Dickinson, Franklin Lakes, NJ), which were placed in a 24-well tissue culture plate containing 500 μl of the medium supplemented with or without graded doses (0–100 ng/ml) of CCL3, CXCL9 (R&D systems), CXCL12 (22) and CCL21 (6). Four hours later, cells in the bottom of each well were collected and counted as previously reported (6).

### *HEV-binding assay*

A modified Stamper–Woodruff assay (*ex vivo* HEV-binding assay) was performed as described (23,24). In brief, 6 μm frozen sections were pretreated with 100 μl mAb against homing-associated molecules or control for 20 min at 4°C. In some experiments, pDC precursor cell suspension was pretreated with 100 μl of anti-L-selectin mAb for 20 min at 4°C. Cryosections were overlaid with cell suspensions ($5 \times 10^5$ cells in 100 μl) and incubated at room temperature for 30 min with horizontal rotation at 60 r.p.m. We confirmed microscopically that non-binding cells did not show decreased viability or increased cellular aggregation during the experiment. After fixation, target tissues were immunostained for PNAd and ALP-labeled streptavidin (Zymed Laboratory Inc., San Francisco, CA). Assays were performed using MACS-sorted $CD11C^+$ DC precursors, a 1:1 mixture of biotin-labeled pDC precursors and non-labeled $CD3^+$ T lymphocytes, and MACS-sorted pDC precursors treated with function blocking Abs or control Abs. All adhesion assays were performed at least five times, and at least 100 HEVs were scored per sample.

### *Short-term homing assay*

An adoptive transfer assay, also called a short-term homing assay, was performed as described (6). In brief, blood cells were collected from 20 *P. acnes*-primed mice or 50 naive mice at day 3 and MACS-sorted, $CD11c^+$ non-separated cells, $B220^-CD11c^+$ or $B220^+CD11c^+$ cells were labeled with 2.5 μM carboxyfluorescein succinimidyl ester (CFSE, Molecular Probes Inc., Eugene, OR) for 10 min at 37°C, and transferred i.v. into syngeneic one naive or *P. acnes*-primed mouse on day 3. Two hours later, host tissues were examined by immunohistochemical staining.

In some experiments, MACS-sorted, blood $MHCII^-CD11c^+$ cells ($4 \times 10^6$) were labeled with 5 μM of 5-(and-6)-([(4-chloromethyl)benzoyl]amino) tetramethylrhodamine (CMTMR, Molecular Probes Inc.) for 15 min at 37°C and transferred into *P. acnes*-primed mice on day 2. Thirty and sixty minutes later, mice were sacrificed for lectin staining and LN tissues were examined. Lectin staining and perfusion fixation of vasculature were performed as described (25). Mice were anesthetized with ketamine (87 mg/kg) plus xylazine (13 mg/kg) injected intramuscularly. FITC-labeled *Lycopersicon esculentum* lectin (100 μg in 100 ml of 0.9% NaCl; Vector Laboratories, Burlingame, CA) was injected into the tail vein and allowed to circulate for 2 min before perfusion of fixative. The vasculature was perfused for 3 min at a pressure of 120 mmHg with 4% paraformaldehyde–PBS from an 18-gauge cannula inserted into the aorta via an incision in the left ventricle. After removal, tissues were stored in 4% paraformaldehyde–PBS at 4°C for 2 h, infiltrated overnight with 30% sucrose, frozen, and cut with a cryostat. Ten or fifty micrometer-thick tissue sections were rinsed with PBS,

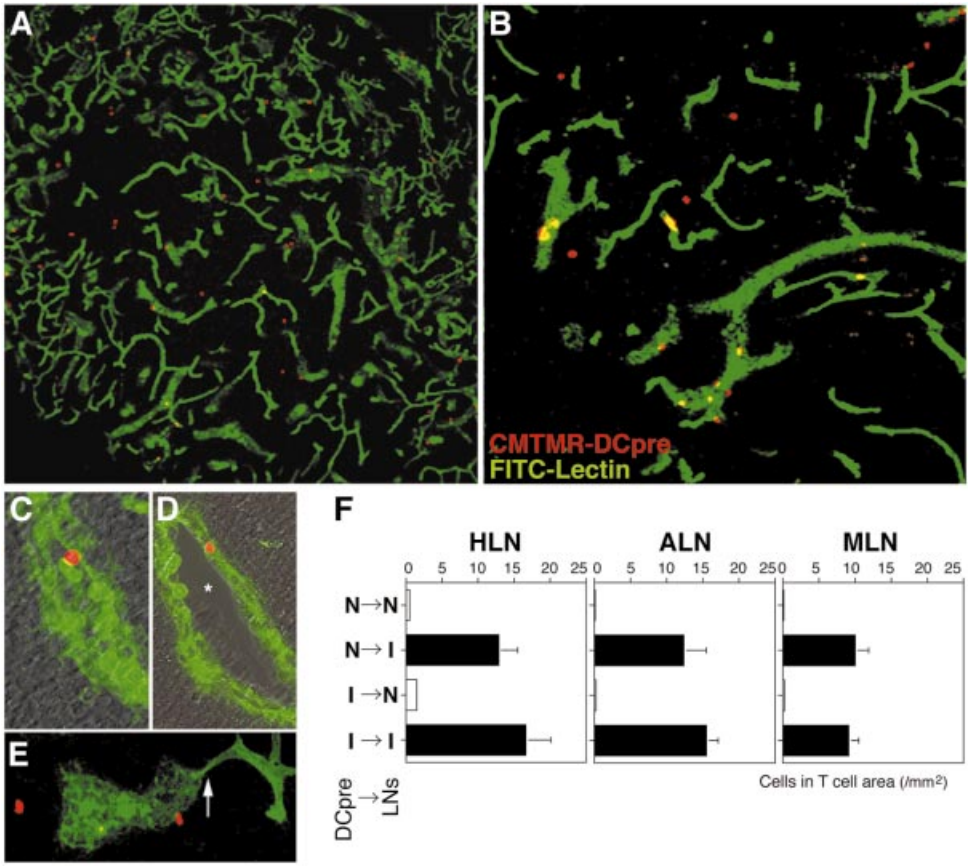


**Fig. 1.** Trans-HEV migration of DC precursors to inflamed LNs. (A–E) CMTMR-labeled, MACS-sorted CD11c$^+$ DC precursors (red) enter *P. acnes*-primed PLNs on day 2 through FITC-lectin$^+$ (green) 'round' HEVs, but not capillaries, 30 min (A and C) and 60 min (B, D and E) after adoptive transfer. Note that many transferred DC precursors (red) enter the tissue space (A, B and E). DC precursors attach on the luminal surface of HEVs (C), transmigrate through HEVs (D), and extravasate to the tissue space of the paracortex (E). Asterisk (D), lumen; arrow (E), border between capillary and HEV; 50 μm-thick section (A and B); 10 μm-thick section (C–E); ×10 (A), ×20 (B), ×63 (C and D), ×50 (E). (F) Increased migration of naive (N) and inflammation-associated (I) CD11c$^+$ DC precursors (DCpre) into *P. acnes*-primed LNs (I) on day 3 (black bars) and naive (N) LNs (white bars). Data are expressed as the number of CFSE$^+$ cells in T cells areas (mm$^2$) of the LNs. HLN, hepatic LN; ALN, axillary LN; MLN, mesenteric LN. Representative data from three independent experiments. Mean ± SD ($n$ = 5 recipients).

mounted in Vectashield (Vector Laboratories), and examined with a Leica TCS-SL laser-scanning confocal microscope.

### *Statistical analysis*

Differences were evaluated using the Student's *t*-test. $P < 0.05$ was considered to be statistically significant.

## Results

### *Only precursor stage of DCs undergoes trans-HEV migration into inflamed LNs*

To determine whether DCs transmigrate across HEVs directly from the circulation, a short-term homing assay was performed in naive mice (N) or mice infected with heat-killed *P. acnes* at day 2 (I). Either normal mouse-derived blood MHCII$^-$CD11c$^+$ DC precursors (N), *P. acnes*-primed mouse-derived blood MHCII$^-$CD11c$^+$ DC precursors (I), normal liver-derived MHCII$^+$CD11c$^+$ immature DCs or granuloma-laden liver-derived MHCII$^+$CD11c$^+$ mature DCs (6) were adoptively transferred after CMTMR-labeling and their distributions were traced. MHCII$^-$CD11c$^+$ DC precursors had attached to and transmigrated across LN HEVs, and extravasated to tissue spaces of the paracortex and perifollicular area 1 h after cell transfer (Fig. 1A–E, and Supplementary Movie, available at *International Immunology* Online). DC precursors obtained from both naive (N) and inflamed (I) mice preferentially migrated into HEVs of inflamed but not naive LNs (Fig. 1F). In addition, these precursors also entered the non-draining LNs of systemically inflamed hosts (Fig. 1F). MHCII$^+$CD11c$^+$ immature and mature DCs showed minimal entry into LNs directly from the circulation (data not shown), as consistent with previous reports (2). These findings indicate that only the precursor stage of DCs transmigrates across HEVs if host LNs are inflamed.

### *Characterization of two subsets of circulating DC precursors*

To identify the fraction undergoing trans-HEV migration, the properties of blood DC precursors obtained from naive and *P. acnes*-primed mice were characterized. Murine blood MHCII$^-$CD11c$^+$ cells are classified into two subsets: B220$^-$CD11c$^+$ mDC precursors and B220$^+$CD11c$^+$ pDC precursors

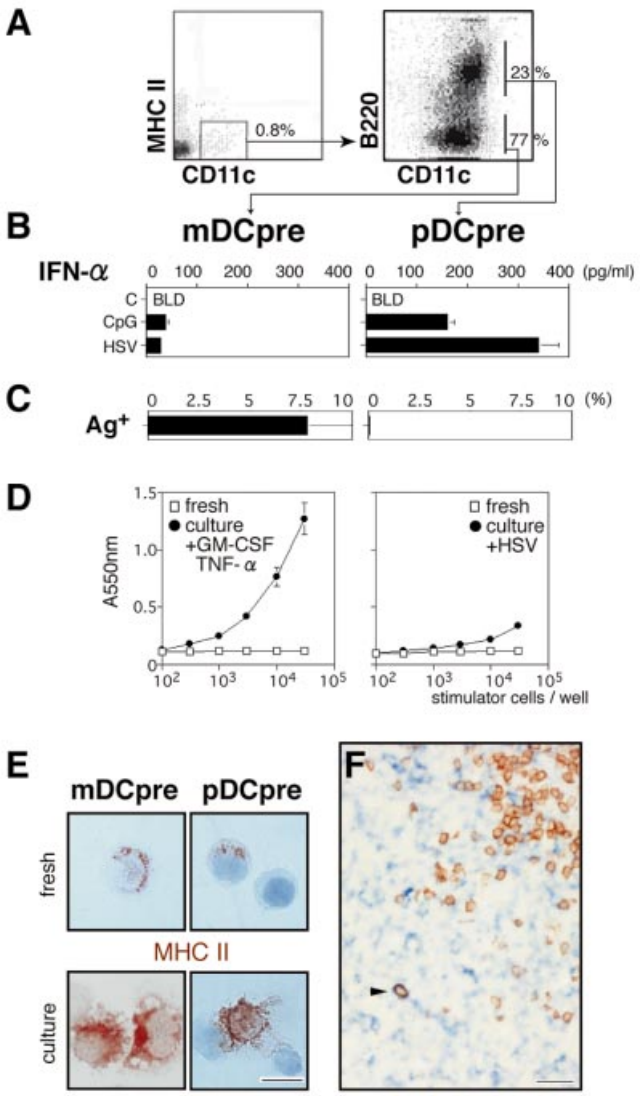


**Fig. 2.** Characterization of two subsets of circulating DC precursors. (A) FACS assay of B220 expression on blood MHCII$^-$CD11c$^+$ DC precursors in naive mice. (B) IFN-α production by mDC and pDC precursors stimulated for 24 h with the indicated substance. C, medium alone as negative control; BLD, below detection limit. (C) Percentage of *P. acnes*-positive cells on cytosmear preparations for freshly isolated DC precursors of both types obtained from *P. acnes*-primed mouse blood at day 1. (D) Primary allogeneic MLR of freshly isolated or cultured DC precursors of both types. Scale bar, 10 μm. (E) Morphology and MHCII-staining (brown) of freshly isolated (upper panels) and cultured (lower panels) mDC (left) and pDC (right). (F) Morphology of mDC (blue) and pDC (black, arrowhead) in normal hepatic LNs. B220 (brown) and CD11c (blue) staining. Scale bar, 20 μm.

(6,26). Twenty-three percent of the MHCII$^-$CD11c$^+$ cells from naive mice (Fig. 2A) and 25% from *P. acnes*-primed mice (6) were B220$^+$ cells, confirmed as pDC precursors by their ability to produce IFN-α after stimulation with CpG or herpes simplex virus (HSV) (Fig. 2B). Functionally, freshly isolated mDC precursors showed phagocytotic activity (Fig. 2C) and acquired antigen presenting cell (APC) function after culture with GM-CSF plus TNF-α on type-I collagen plates (Fig. 2D). In contrast, we could not detect *P. acnes*-laden cells (Fig. 2C) or APC function in pDC precursors (Fig. 2D). Freshly isolated mDC- and pDC-precursors exhibited monocyte-like morphology but could be distinguished by cell size (Fig. 2E). Both subsets were cell surface MHCII-negative but include this molecule within their cytoplasm (Fig. 2E). After culture, most DCs acquired dendritic-shape with cell surface MHCII (Fig. 2E). While mDCs also showed dendritic-shape *in situ*, we could not detect dendritic-shaped pDCs (Fig. 2F) in naive as well as inflamed LNs.

### *Homing-associated molecules on two subsets of circulating DC precursors*

We examined the leukocyte homing-associated molecules present on freshly isolated DC precursors. Expression of adhesion molecules showed similar patterns between both precursors except for L-selectin and αE-integrin, which were preferentially detected in pDC- and mDC precursors (Fig. 3A), respectively. Both DC precursor types expressed similar chemokine receptor mRNAs such as CCR1, CCR5 and CXCR4 (Fig. 3B). Whereas mDC precursors highly expressed CCR1 and CCR5 mRNAs, pDC precursors additionally expressed CXCR3 mRNAs (Fig. 3B). CCR7 mRNA was up-regulated in both subsets after stimulation (Fig. 3B, C-DC). The relative levels of chemokine receptor mRNAs were similar in naive and *P. acnes*-induced blood DC precursors (N-DCp and I-DCp; Fig. 3B). In chemotaxis assays, mDC precursors were strongly attracted by CCR1/5-ligand CCL3 (Fig. 3C); pDC precursors also migrated toward CXCR3-ligand CXCL9/Mig in a dose-dependent manner (Fig. 3C). After short-term culture, the responsiveness to CCL3 and CXCL9 was reduced while that to CCR7-ligand, CCL21, of both DCs was increased ($0.78 \times 10^3$ cells for fresh mDCpre, $1.12 \times 10^3$ for cultured mDCs; $0.50 \times 10^3$ for fresh pDCpre, $1.15 \times 10^3$ for cultured pDCs; at 10 ng/ml of CCL21) (Fig. 3C). Furthermore, both precursors responded to the CXCR4-ligand, CXCL12/SDF-1, at relatively low concentrations (Fig. 3C), although their expression levels of CXCR4 mRNA (1.9 for I-mDCpre, 1.3 for I-pDCpre, 1.0 for HPRT) were low compared to those of CCR1 (268.7 for I-mDCpre, 90.7 for I-pDCpre, 1.0 for HPRT) and CCR5 (61.9 for I-mDCpre, 38.0 for I-pDCpre, 1.0 for HPRT).

### *Inflammation induces rapid and parallel mobilization of two DC precursors into the circulation*

The numbers of both mDC- and pDC-precursors in naive mouse blood were extremely low, but increased greatly after *P. acnes* injection (Fig. 4). The ratio of blood mDC to pDC precursors was constant at ~3:1 throughout experiments (Figs 2A and 4). Since inflammation-associated DC precursors are important to granuloma formation, and tumor necrosis factor (TNF)-α-blockade or TNFR p55-deficient mice did not develop granulomas (10,18), we tested the effect of neutralizing anti-TNF-α antibody (Ab) on the appearance of blood DC precursors. Blocking TNF-α completely inhibited the *P. acnes*-mediated mobilization of both DC precursors (Fig. 4). In addition, when mice were pretreated with blocking Ab against L-selectin or CXCL12, two major molecules highly expressed by bone marrow progenitor cells (27), mobilization of both precursors was also inhibited (Fig. 4). Thus, intravascular

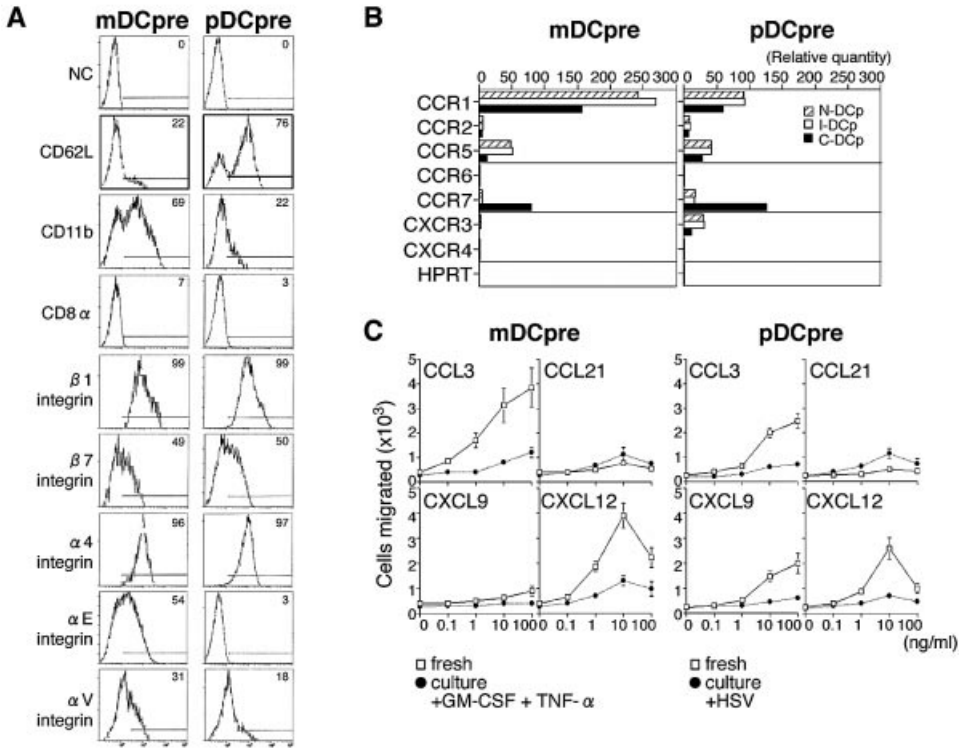


**Fig. 3.** Homing-associated molecules on two subsets of circulating DC precursors. (A) Expression of adhesion molecules by mDC- and pDC-precursors obtained from naive mouse blood. (B) Chemokine receptor expression on blood mDC- and pDC-precursors obtained from naive (N-DCp) or *P. acnes*-inflamed (I-DCp) mice and on cultured DCs (C-DCp; see Methods). (C) Chemotaxis of freshly isolated blood DC precursors and cultured matured DCs against various doses of chemokines. Representative data from five independent experiments shown. Mean ± SD ($n$ = 6).

danger-signals like *P. acnes* readily mobilize both mDC- and pDC-precursors into the circulation in a TNF-α-dependent manner possibly from bone marrow.

### *Inflammation controls chemokine expressions on LN HEVs*

Candidates of LN HEV-associated homing molecules were identified by an immunohistochemical staining together with the L-selectin ligand PNAd, a stable marker for HEVs. E-selectin was barely detected in naive mouse HEVs, but strongly induced and concentrated at the luminal surface of inflamed LN HEVs (Fig. 5A). Based on *in vitro* chemokine-responsiveness (Fig. 3C), the four HEV-associated chemokines were estimated by percentage of merged areas compared to control areas of PNAd-staining. Lymphocyte-homing chemokines (28), CXCL12 (Fig. 5B) and CCL21 were constitutively detected, but dramatically decreased in area on day 2 of infection (Fig. 5C, E and G). In contrast, CXCL9 was marginally detected at the luminal side of a small subset of normal HEVs, but its expression was increased after *P. acnes* administration (Fig. 5F and G). CCL3 was also induced by *P. acnes*, but the expression levels were low (Fig. 5D and G). When mice were pretreated with neutralizing Ab against TNF-α, increased expressions of CXCL9 and E-selectin on HEVs of not only draining HLNs but also non-draining ALNs and MLNs were inhibited (Fig. 5H).

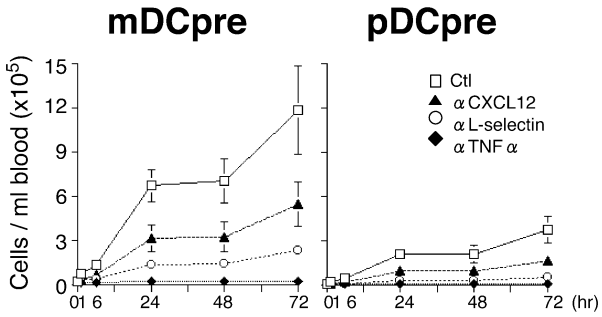


**Fig. 4.** Rapid mobilization of mDC- and pDC-precursors into the circulation in response to intravascular danger signal. The number of blood mDC- and pDC-precursors after *P. acnes* injection, and the effects of blocking Abs against CXCL12, L-selectin and TNF-α or control Ab (Ctl) on the mobilization of DC precursors in the circulation.

### *pDC precursors bind to inflamed LN HEVs*

To directly demonstrate whether DC precursors can bind to LN HEVs as a prerequisite for transmigration, we performed *ex vivo* HEV-binding assay (Fig. 6A). A considerable number of MACS-sorted CD11c$^+$ DC precursors actually bound to both draining and non-draining LN HEVs. By calculating the percentage of DC precursor-bound HEVs, we found that

both naive (N) and *P. acnes*-induced (P) DC precursors preferentially bind to inflamed over naive HEVs (Fig. 6B). This result indicates that activation of host HEVs, is crucial for DC-HEV binding. When mDC or pDC precursors were tested separately, pDC precursors, but not mDC precursors and liver MHCII$^+$CD11c$^+$ DCs, bound to LN HEVs (Fig. 6C).

When we pre-treated pDC precursors with Abs to L-selectin, or inflamed sections with Abs to E/P-selectin and chemokines, combined blockade of CXCL9 and E-selectin dramatically decreased the absolute number of HEV-bound pDC precursors (Fig. 6C). When we pre-treated a 1:1 mixture of pDC precursors and CD3$^+$ T lymphocytes with Abs to CXCL9 or E-selectin, we observed a significant decrease in the ratio of HEV-bound pDC precursors to lymphocytes (Fig. 6D). In contrast, Abs to CCL21, CXCL12 and L-selectin increased the ratio of pDC/lymphocytes (Fig. 6D). Thus, CXCL9 and E-selectin are preferentially involved in pDC precursor binding to LN HEVs, while CCL21, CXCL12 and L-selectin are lymphocyte tropic HEV-homing molecules.

### *pDC precursors transmigrate inflamed HEVs*

Because DC precursors from naive and inflamed mice were indistinguishable in phenotype, function, chemokine receptor expression and migratory behavior (Figs 2 and 3), we used *P. acnes*-mobilized blood DC precursors in the following experiments to obtain a sufficient number of cells, unless otherwise indicated. Two subsets of DC precursors were separately transferred *in vivo* (Fig. 7). mDC precursors predominantly migrated into the liver sinusoids (6), marginal zone of the spleen, and to a lesser extent, the skin dermis and gut epithelium (Fig. 7). Even when transferred to *P. acnes*-primed mice, these cells never entered the LN via HEVs. A few cells, however, were detected in the subcapsular sinus of hepatic LNs (not depicted), suggesting their entry into the LNs through the liver and afferent lymphatics as described in our previous study (6,23). In contrast, isolated pDC precursors rarely entered the peripheral tissues (Fig. 7), but selectively migrated into both draining hepatic and other non-draining secondary LNs (Fig. 7) when the hosts were systemically inflamed.

### *HEV-CXCL9 determine transmigration of pDC precursors*

Various blocking Abs were injected i.v. just prior to pDC precursor transfer. Pretreatment with anti-CXCL9 polyclonal Ab (pAb) alone or with anti-E-selectin monoclonal Ab (mAb) significantly inhibited accumulation of pDC precursors in non-draining LNs (Fig. 8A). In contrast, treatment with Abs to CCL3, the most potent chemokine recruiter of mDC precursors into the liver (6), had no effect (Fig. 8A). Distinct from naive lymphocytes which enter the LNs through L-selectin and CCR7, pDC precursors are less dependent on L-selectin and CCL21 in migration into the LNs (Fig. 8A). Anti-CXCL12 Ab was also ineffective (Fig. 8A) as expected from the reduction of CXCL12$^+$ HEVs in inflammation (Figs. 5G). We also tested the migration of pDC precursors collected from CXCR3-deficient (CXCR3$^{-/-}$) mice. Mobilization of blood pDC precursors by *P. acnes* into the circulation was not impaired (data not shown). When we transferred CXCR3$^{-/-}$ pDC precursors, the numbers of HEV-associated cells, especially extravasated cells were significantly decreased (Fig. 8B), confirming that CXCR3 is necessary for trans-HEV migration by pDC precursors.

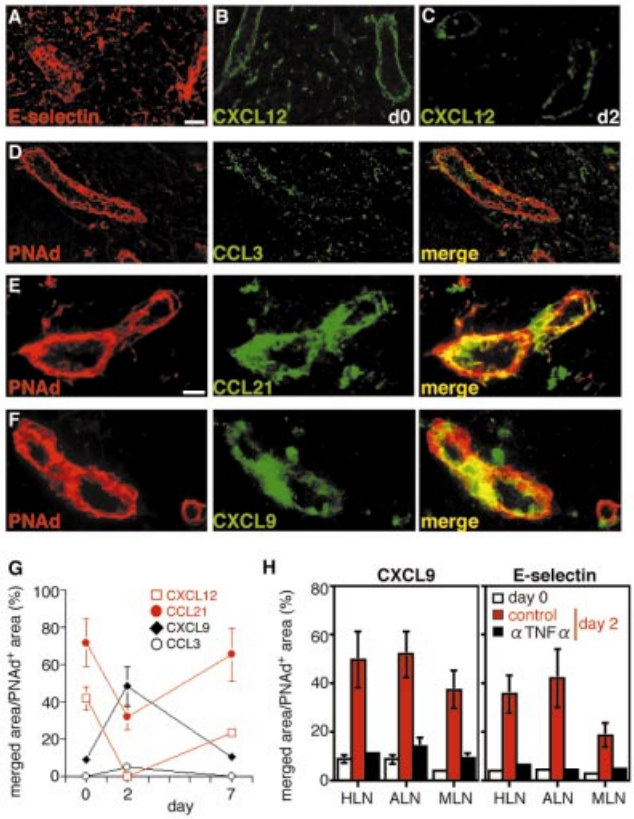


**Fig. 5.** Kinetics of activation molecules on HEVs. (A–F) Immunostaining of HLN HEVs on day 0 (B) and 2 (A and C–F) after *P. acnes* injection. (A) E-selectin (red). (B and C) CXCL12 (green). (D) PNAd (red), CCL3 (green) and merged (yellow). (E) PNAd (red), CCL21 (green) and merged (yellow). (F) PNAd (red), CXCL9 (green) and merged (yellow). Scale bars, 40 μm (A–C), 20 μm (D–F). (G) Kinetics of percentages of merged areas to PNAd$^+$ areas calculated by IPLab software. (H) Effect of anti-TNFα Ab or control Ab on the percentage for areas of CXCL9$^+$ or E-selectin$^+$ PNAd.

### *Local HSV infection also induces parallel mobilization of DC precursors and activates LN HEVs*

The two inflammation-associated DC precursors undergo distinct trafficking pathways in response to an intravenous danger signal, as pDCs directly enter the LNs without scanning local inflamed tissues. We next investigated whether DC precursors undergo such a pathway in a local danger-signal model, and traced their trafficking in a cutaneous HSV-1 infection model (29). Local infection in the right (rt.) footpad increased serum TNF-α levels, with two peaks at 1 h and 2 days after HSV injection (Fig. 9A), indicating that cutaneous infection also induced systemic reactions. A significant number of mDC- and pDC-precursors were mobilized into the circulation on day 2 (Fig. 9B), both of which possessed similar patterns for chemokine receptor mRNAs (Fig. 9C) compared to *P. acnes*-mobilized DC precursors (Fig. 2B). Enhanced expression of CXCL9 and E-selectin was observed in draining rt. popliteal LN (PLN) and also non-draining LN

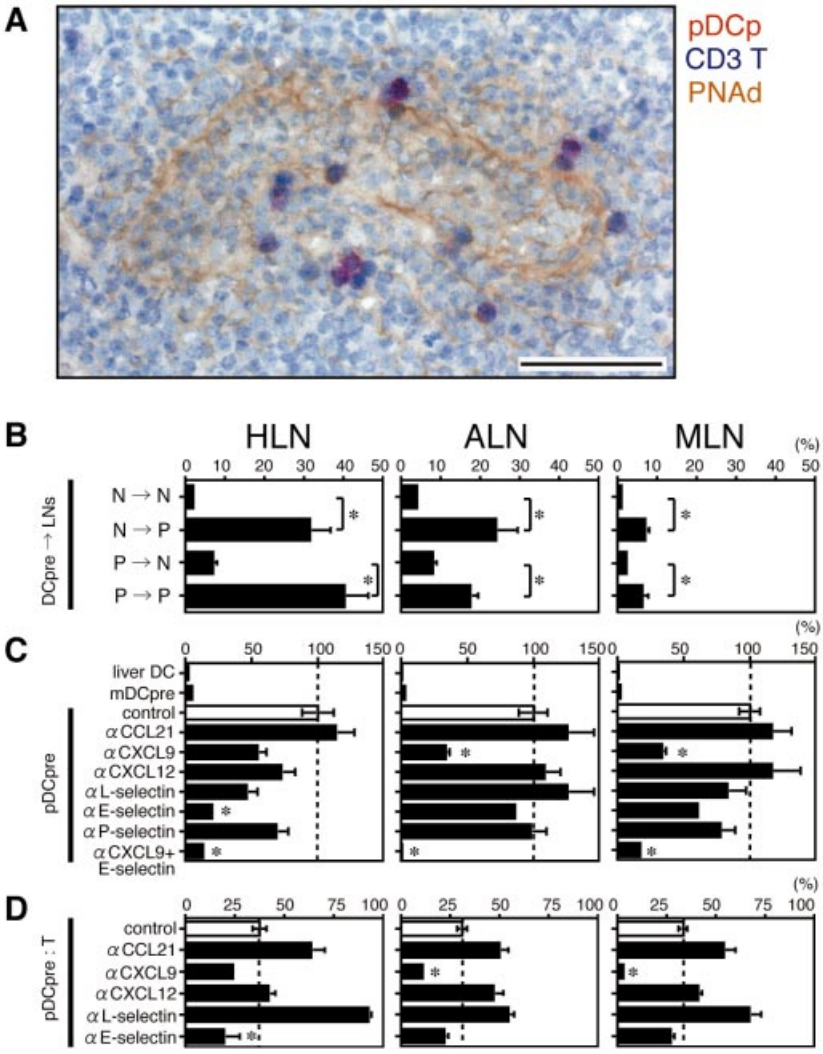


**Fig. 6.** pDC precursors bind to inflamed LN HEVs. *Ex vivo* HEV-binding assay. (A) pDC precursors (red) and CD3+ T cells (dark blue) attached to inflamed axillary LN HEVs (PNAd, brown). Scale bar, 100 μm. (B) MACS-sorted CD11c+ DC precursors obtained from naive (N) and *P. acnes*-primed mice on day 2 (P) were overlaid on three LN cryosections obtained from naive (N) and *P. acnes*-primed mice on day 2 (P). Data are expressed as percent DC precursor-bound HEVs. (C) Effect of blocking Abs on pDC precursor binding to LN HEVs. Isolated mDC- and pDC-precursors and liver MHCII+CD11c+ DCs are shown. Data are expressed as percent inhibition of HEV-bound DC precursors compared with control Ab. (D) Ratio of bound pDC precursors to CD3+ T lymphocytes. Representative data from five independent experiments. Mean ± SD ($n$ = 6). *$P$ < 0.05 by Student's $t$-test; Significance calculated for each LN.

HEVs on day 2, and decreased thereafter (Fig. 9D). DC mobilization and HEV-chemokine enhancement were efficiently inhibited by blocking TNF-α (Fig. 9B and D). While blockade of CXCL9 plus E-selectin did not affect DC precursor mobilization into the circulation in response to local HSV infection, blocking CXCL12 or L-selectin again decreased the number of both DC precursors (Fig. 9B).

### *Rapid recruitment of mDC- and pDC-precursors to distinct sites after local HSV infection*

Accelerated influx of CD11c+ cells to the dermis was observed around the HSV-injected site on day 1 of infection (Fig. 10A and B). Newly appeared dermal CD11c+ cells were B220-negative in tissue sections (Fig.10B) and kinetically distinct from previously reported CD11c− monocytes (30), indicating

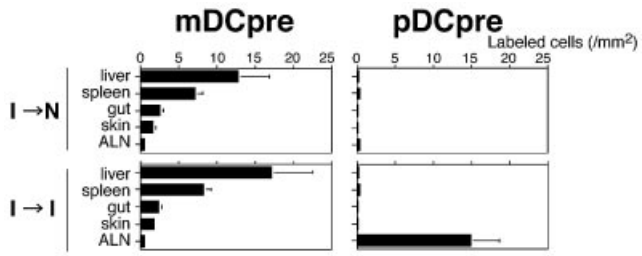


**Fig. 7.** Distinct trafficking of mDC- and pDC-precursors. mDC- and pDC-precursors were separately isolated from *P. acnes*-primed mice (I→), labeled with CFSE, and transferred into normal (→N) and *P. acnes*-primed (→I) mice at day 2. Data are expressed as the number of CFSE+ cells (/mm²) of the indicated tissues 2 h after cell transfer. 15 mm² sections were counted ($n$ = 3 recipients).

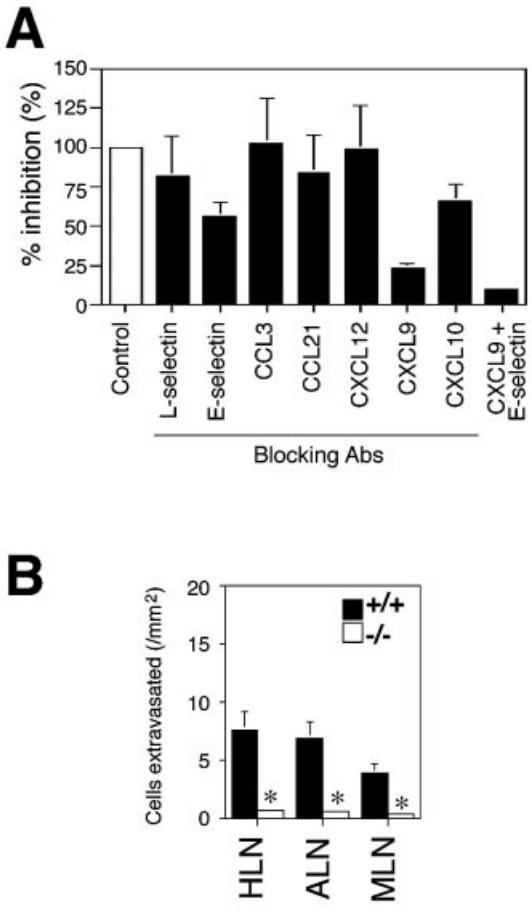


**Fig. 8.** HEV-CXCL9 determines transmigration of pDC precursors. (A) Effect of anti-chemokine and anti-selectin Abs on direct transmigration of pDC precursors into *P. acnes*-primed, non-draining ALNs at day 2. Data from three independent experiments are expressed as % inhibition compared to control. Mean ± SD ($n$ = 6). (B) The number of donor wild-type (+/+) and CXCR3-deficient (–/–) pDC precursors that extravasated into *P. acnes*-primed HLNs, ALNs and MLNs at day 2. One hour after cell transfer. Representative data from two independent experiments. Mean ± SD ($n$ = 3). *$P < 0.05$ by Student's $t$-test.

these cells to be mDC precursors recruited to inflamed skin. CD11c$^+$ cells simultaneously increased in number and accumulated at HEVs near follicles of rt. PLN (Fig. 10B and C) as well as lt. PLN, bilateral ALNs, HLNs and MLNs (data not shown) in parallel with HEV-chemokine expression patterns (Fig. 9C). We also observed that 81.4 ± 17.3% ($n$ = 10, 15 mm$^2$ section/mouse) of CD11c$^+$ DCs within the luminal side of HEVs were B220-positive (Fig. 10B and D).

When we adoptively transferred blood mDC precursors i.v. into HSV-infected mice at day 2, their entry to the skin of the rt. inflamed footpad was partially inhibited by anti-CCL3 Ab, but not by anti-CXCL9 plus E-selectin Abs (Fig. 11A). When we transferred pDC precursors, combined blockade of CXCL9 and E-selectin almost completely inhibited LN entry of these cells, but blockade of CCL21 did not (Fig. 11A). CXCR3$^{-/-}$ mice-derived pDC precursors again failed to enter the paracortex of LNs when transferred into HSV-infected mice at day 2 (Fig. 11B). Therefore, similar mobilizing and trafficking patterns were observed between intravenous *P. acnes* and local HSV infection models.

## Discussion

Transendothelial migration of leukocytes is regulated by complex processes such as heterogeneity in microvillus length (31), glycosylation (32), and the concentration of homing molecules on the tip of cells (33). Chemokines contribute to at least two steps of leukocyte transmigration, adhesion and diapedesis, by activating integrin and forming chemotactic gradient together with glycosaminoglycan (28,32). Since chemokine receptor mRNA expression levels on leukocytes are not always consistent with their chemotaxis toward the corresponding ligands, we performed *ex vivo* binding and short-term homing assay using neutralizing Abs to conclude the *in vivo* role of chemokines in DC precursor trafficking. CXCL12 has been reported *in vitro* to attract bone marrow-derived, cultured mouse pDCs (34) and human blood pDCs (35). We also confirmed that pDC precursors respond to CXCL12 *in vitro* (Fig. 3C) as well as in mobilizing DC precursors into the circulation (Figs 4 and 9B). However, CXCL12-blockade did not inhibit trans-HEV migration of pDC precursors (Fig. 8A), possibly due to the significant reduction of CXCL12 in inflamed HEVs on day 2 (Fig. 5G). This pattern is similar to that of fucosyltransferase-VII, which is constitutively expressed in adult LN HEVs and biosynthesizes L-selectin ligands to mediate L-selectin-dependent lymphocyte homing, but transiently disappears following antigenic stimulation (36). Another L-selectin ligand, GlyCAM-1 was also reported to show similar reduction (37). The significance of inflammation-induced transient reduction of L-selectin ligands and CXCR4 ligand remains unknown, but might be helpful for pDC precursors competing for access to inflamed HEVs, as lymphocytes are still the major population observed in inflamed LN HEVs (data not shown; see also Fig. 10D which depicts preferential detection of B cells over pDC precursors within LN HEVs). Or, increased ratio of CXCL9 to CXCL12 may provide an appropriate condition for pDCs to undergo transendothelial migration (35).

L-selectin is also believed to induce blood-borne migration of pDCs to LNs, since the number of LN pDCs is decreased in L-selectin-deficient mice (38) and by the treatment with anti-L-selectin Ab in a mouse mammary tumor virus infection model (39). However, these reports did not directly prove that DCs actually transmigrate across HEVs through L-selectin. As L-selectin is also involved in the mobilization of hematopoietic progenitor cells between the bone marrow and peripheral blood, and in the recruitment of leukocytes to peripheral inflamed tissues (32), L-selectin neutralization and gene-knockout may affect multiple steps of pDC recruitment. In *P. acnes*- and HSV-infection, L-selectin-blockade inhibited the mobilization of both DC precursors into the circulation (Figs 4 and 9B) but not the trans-HEV migration of pDC precursors (Fig. 8A). We consider that both L-selectin and CXCL12 are preferentially involved in the mobilization of DC precursors into the circulation, possibly due to high expressions of CXCR4 and L-selectin on bone marrow progenitors/precursors.

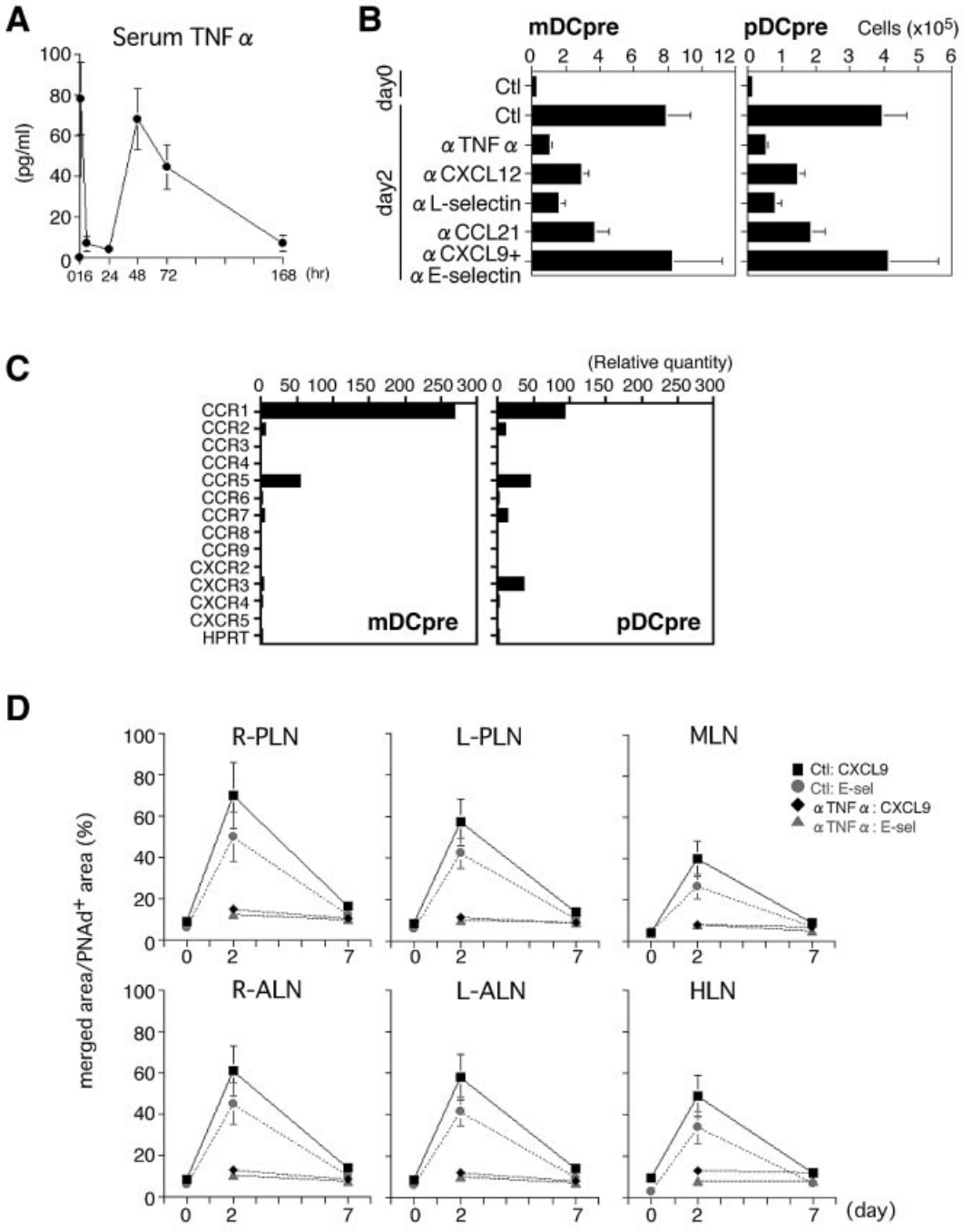


**Fig. 9.** Mobilization of mDC- and pDC-precursors and HEV-activation in local HSV infection. (A) Kinetics of serum TNF-α. (B) The number of blood mDC- and pDC-precursors on day 0 and 2 after rt. footpad infection. Control Abs (Ctl) and blocking Abs against TNF-α, CXCL12, L-selectin, CCL21 and CXCL9 plus E-selectin were injected i.v. just prior to HSV infection. Representative data from three independent experiments. Mean ± SD ($n$ = 6). (C) Expression profiles for chemokine receptor mRNAs on freshly isolated mDC- and pDC-precursors at day 2 of infection. (D) Kinetics of staining for HEV-CXCL9 and E-selectin in various LNs and the effect of anti-TNF-α Ab. Percentages of merged areas to PNAd$^+$ areas were calculated by IPLab. R, right; L, left. Representative data from three independent experiments. Mean ± SD ($n$ = 6).

CCL21 did not affect LN entry by blood pDC precursors in this study (Figs 8A and 11). This is not simply due to decreases in CCL21$^+$ HEVs (Fig. 5G), because there was minimal migration of CCR7$^+$ mature DCs across HEVs (data not shown) with constitutive expression of CCL21 at high levels despite their chemotactic response to CCL21 *in vitro* (Fig. 3C). We speculate that CCR7 may be preferentially used by mDCs when migrating from peripheral tissues to draining LNs through CCL21$^+$ afferent lymphatics. The difference in selectin and chemokine-dependency between DCs and lymphocytes

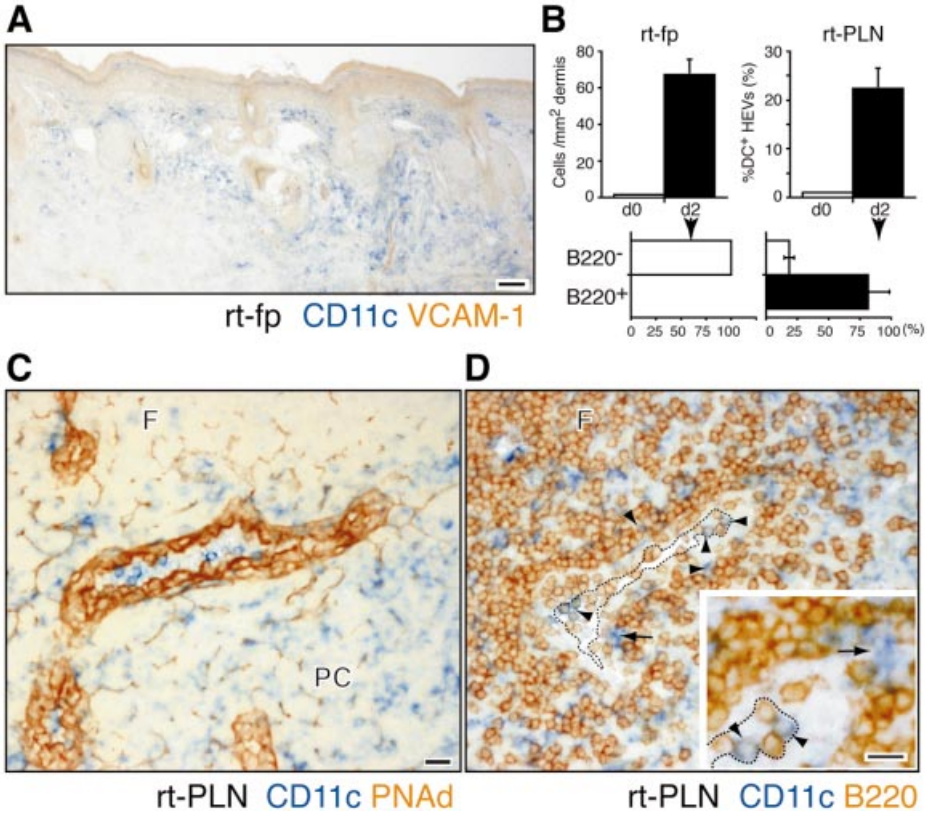


**Fig. 10.** Distinct recruitment of mDC- and pDC-precursors in HSV infection. (A) Immunostaining for CD11c (blue) and VCAM-1 (brown) of rt. footpad 1 day after HSV infection. Note that many CD11c⁺ cells accumulate around the site of HSV injection in the dermis. Scale bar, 100 μm. (B) The number of CD11c⁺ cells in rt. dermis (upper left) and percentage of CD11c⁺ DC-positive HEVs in rt. PLNs (upper right) on day 2 (black bars) and in naive LNs (white bars). Percentage of B220⁺ cells among above CD11c⁺ cells (see also D) on day 2. For dermal cell count, an area of 1.5 × 1.5 $cm^2$ at site of injection (day 1) or the corresponding area (day 0) was excited. Representative data from three independent experiments. Mean ± SD ($n$ = 5). (C) Immunostaining for CD11c (blue) and PNAd (brown) of rt. PLN 2 days after HSV infection. 'Round' CD11c⁺ cells were detected within the lumen of HEVs located near follicle. (D) Immunostaining for CD11c (blue) and B220 (brown) of rt. PLN 2 days after HSV infection. Note that HEV-attached CD11c⁺ cells were double positive cells (black, arrowheads). Dotted outline shows the luminal surface of HEV near follicle. Although CD11c-single positive 'dendritic'-shaped cells (arrow) are also detected outside HEVs, this does not always mean trans-HEV migration. Scale bar, 40 μm; 15 μm (insert). F, follicle; PC, paracortex.

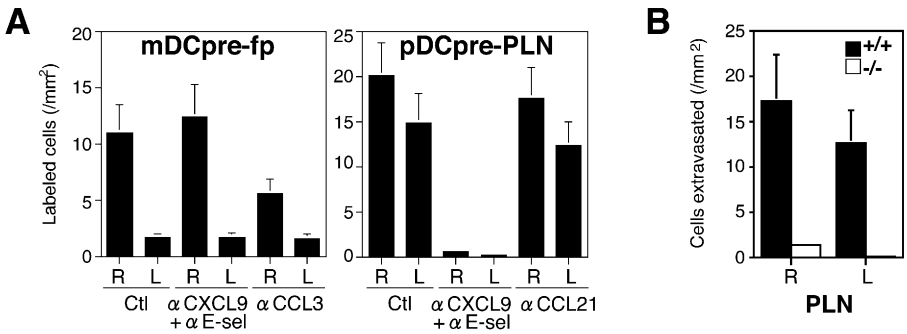


**Fig. 11.** CXCL9 and CXCR3-driven recruitment of pDC-precursors in HSV infected LNs. (A) The number of CFSE-labeled mDC precursors and pDC precursors detected at day 2 footpad (left) and PLN (right) respectively. Twenty minutes after labeled cell transfer. Control and blocking Abs against CXCL9 plus E-selectin, CCL3 and CCL21 were injected i.v. 1 h prior to cell transfer. Representative data from three independent experiments. Mean ± SD ($n$ = 3 recipients). (B) The number of donor wild-type (+/+) and CXCR3-deficient (–/–) pDC precursors that extravasated into HSV-infected PLNs at day 2. One hour after cell transfer. Representative data from two independent experiments. Mean ± SD ($n$ = 3 recipients). *$P$ < 0.05 by Student's $t$-test.

might also be due to distinct cell morphology and carbohydrate epitopes.

pDC precursors also express CCR1 and CCR5 (Fig. 3B), but did not use them for trans-HEV migration as expected by the very low expression of HEV-CCL3 (Figs 5G and 8A). We have recently established that CCR1/CCR5 and CCL3 are pivotally involved in the mobilization of both mDC- and pDC-precursors into the circulation in *P. acnes* infection (40). It is interesting that both mDC- and pDC-precursors appear in the circulation at a ratio of ~3:1 (Figs 2A, 4 and 9B) showing similar chemokine receptor mRNA expression profiles such as CCR1, CCR5, CXCR4, and the expression levels are 1.5–3 times higher on mDC precursors (mDC:pDC ratio is 2.98 for CCR1, 1.63 for CCR5, 1.51 for CXCR4; Figs 3B and 9C). This may account for the similar mobilizing pattern of both precursor cell types from the bone marrow into the blood possibly controlled by such chemokine receptors.

CXCR3 is preferentially expressed by pDC subtypes (12,35), but direct evidence for CXCR3-mediated trans-HEV migration has not been shown. Our short-term homing assay using CXCR3$^{-/-}$ mice-derived pDC precursors as well as CXCL9 blockage clearly demonstrates the necessity of CXCR3–CXCL9 interaction for pDC precursors to enter the tissue spaces of LNs in bacterial and viral infection. CXCL9 blockage also inhibits DC-HEV binding (Fig. 6C), suggesting that CXCL9–CXCR3 interaction also provides activation signals to pDC precursors for subsequent arrest and diapedesis. LN-recruitment of pDC precursors is controlled not only locally but also systemically, as CXCL9 and E-selectin expressions are TNF-α-dependent (Figs 5H and 9D). In this respect, a small subset of monocytes was reported to undergo blood-borne migration to draining LNs in response to sole adjuvant in a TNF-α and CXCL9-dependent manner (41). Although the fate of LN-recruited monocytes and pDCs in a pathological condition is still unexplored, it is intriguing to speculate that the host defense system rapidly needs monocyte- and DC-lineage cells in the LNs in response to danger signals. We conclude that CXCR3 and an undefined E-selectin-ligand may license pDC precursor-homing to LNs *in vivo*, and that danger signal-dependent HEV-CXCL9 expression is crucial for inducing the trans-HEV migration of these cells.

In our transfer experiments, pDC precursors rarely migrated to peripheral tissues or spleen (Fig. 7) in spite of their presence in these tissues in steady state conditions (38). This discrepancy can be explained as follows. Firstly, most of the blood pDC precursors are a specialized subset for establishing an immunogenic DC system, possibly having distinct origin from resident cells. Or, inflammation-associated pDC precursors are more committed populations compared with previously reported B220$^{+}$CD11c$^{+}$ common DC precursors (13). Secondly, since the detection limit of this experimental system was $2 \times 10^5$ transferred cells, fewer than 10% ($2 \times 10^5/2 \times 10^6$) of the transferred cells could not be detected. This also means that at least 90% of transferred pDC precursors selectively enter the LNs. Thirdly, the spleen lacks HEVs, distinct from LNs. Thus, the homing molecules for immune cell entry to the white pulp, through marginal sinuses, may differ to those of LNs, as the signals activating the HEV-equivalent structures of spleen may also differ from those of LN HEVs.

We mention that we do not negate the possibility that pDC precursors also migrate to peripheral tissues. In short-term homing assay (Figs 8 and 11), we detected increased number of transferred pDC precursors in the host peripheral blood 1 h after blocking CXCL9 plus E-selectin compared to control (data not shown). This suggests the possibilities that circulating pDC precursors who failed to enter the LNs may enter other tissues. However, we could not detect increased number of pDCs in not only the peripheral blood (Fig. 9B) but also other tested peripheral tissues (data not shown) in anti-CXCL9 plus E-selectin Abs-treated, HSV-infected mice at day 2. This may be due to rapid death of pDC precursors during 2 days circulation and to lack of HEV-like structures in peripheral tissues at this time. We speculate that aberrant migration of pDCs to peripheral tissues could occur if survival of pDCs or local environment including endothelial structure and chemokine expression is altered. In this respect, pDCs have been observed in the peripheral tissues in allergy and cancer patients (42), possibly contributing to chronic disease status. Aberrant high expression of CXCL12 was reported to attract pDCs into the tumor sites (43). Also, we cannot completely rule out the presence of other mechanisms regulating a steady state migration of pDC precursors and the contribution of L-selectin, CXCL12 and CCL21 in this process.

In contrast, we could not detect a significant number of mDC precursors in any LNs in our short-term transfer study. One possibility is that transferred mDC precursors were non-specifically trapped in the lung and liver and thus failed to enter the circulation as well as LNs any more. In fact, when we transferred relatively mature DCs, most of these tended to be trapped possibly through non-specific binding (data not shown). However, we consider that tissue-entry of mDC precursors is rather selective due to the following reasons. First, precursor stages of DCs are smaller in size and weaker in adhesiveness compared to mature DCs. Second, transferred mDC precursors, but not mature DCs, were already detected in the peripheral blood (<5%) 30 min after cell transfer, indicating that these precursors passed through the lung and liver but failed to enter the LNs. Third, in *ex vivo* binding assay, mDC precursors selectively bound to hepatic sinusoids, especially Kupffer cells (data not shown). This Kupffer cell-DC binding is mediated by *N*-acetylgalactosamine-specific sugar receptors (44). Moreover, in our previous transfer study (6), when we inhibited mDC precursor traffic to the liver by blocking CCL3, these cells were not detected within the LNs but detectable in the peripheral blood.

We summarize DC precursor trafficking pathway as follows. (i) Danger signals induce local production of TNF-α. (ii) TNF-α released into the circulation promotes systemic inflammation via activation of macrophages and endothelial cells. (iii) Serum TNF-α up-regulates CCL3 and induces mobilization of both mDC- and pDC-precursors (both are positive for CCR1 and CCR5) into the circulation, possibly from bone marrow (both are highly positive for L-selectin and CXCR4). (iv) Serum TNF-α also up-regulates CXCL9 and E-selectin in systemic LN HEVs. (v) mDC precursors are recruited to sites of invasion, capture antigens and consequently migrate into the draining LNs through afferent lymphatics. Local TNF-α accelerates influx of mDC precursors via CCL3 as well as efflux via CCL21

(45). (vi) In contrast, pDC precursors transmigrate across activated HEVs in a CXCL9 and E-selectin dependent manner.

DC precursor traffic in response to danger signals is dynamic, systemically controlled by cytokines, and locally by chemokines. Although pDCs have been reported to flexibly induce TH 1, TH 2 and regulatory types of T lymphocytes like mDCs *in vitro*, the function of pDCs after entering the LNs has not been established *in vivo*. pDCs in LNs never show dendritic morphology distinct from *in vitro* cultured pDCs (Fig. 2), suggesting distinct function from mDCs *in vivo*. It is also interesting that pDC precursors directly migrate to not only draining LNs where antigen-specific immune responses occur, but also to non-draining LNs where such immunity doesn't occur. We speculate that pDCs might flexibly coordinate immune response or tolerance according to LN environment. Further studies for danger signal-recruited pDCs in multiple LNs will help us to understand the mechanism deciding immune response and tolerance.

## Supplementary data

Supplementary data are available at *International Immunology* Online.

## Acknowledgements

We are very grateful to Dr T. Kaburaki (The University of Tokyo) for providing KOS-HSV, to Dr Y. Eishi (Tokyo Medical and Dental College) and to Drs N. Matsuo, Y. Wang, A. Nakano and E. Tohda for their kind assistance. This work was supported in part by Solution Oriented Research for Science (SORST), by the Japan Science and Technology Corporation (JST) and by a grant from Ministry of Education, Culture, Sports, Science and Technology (MEXT).

## Abbreviations

| | |
|---|---|
| ALN | axillary lymph node |
| APC | antigen-presenting cell |
| CCR | CC-chemokine receptor |
| CXCR | CXC-chemokine receptor |
| DC | dendritic cell |
| HEV | high endothelial venule |
| HLN | hepatic lymph node |
| HSV | herpes simplex virus |
| LN | lymph node |
| Mig | monokine induced by gamma interferon |
| MIP | macrophage inflammatory protein |
| MLN | mesenteric lymph node |
| PLN | popliteal lymph node |
| PNAd | peripheral node addressin |
| SDF | stromal cell-derived factor |
| SLC | secondary lymphoid organ chemokine |

## References

1 Banchereau, J., Briere, F., Caux, C., Davoust, J., Lebecque, S., Liu, Y. J., Pulendran, B. and Palucka, K. 2000. Immunobiology of dendritic cells. *Annu. Rev. Immunol.* 18:767.
2 Kupiec-Weglinski, J. W., Austyn, J. M. and Morris, P. J. 1988. Migration patterns of dendritic cells in the mouse. Traffic from the blood and T cell-dependent and -independent entry to lymphoid tissues. *J. Exp. Med.* 167:632.
3 Steinman, R. M. and Pope, M. 2002. Exploiting dendritic cells to improve vaccine efficacy. *J. Clin. Invest.* 109:1519.
4 Butcher, E. C. and Picker, L. J. 1996. Lymphocyte homing and homeostasis. *Science* 272:60.
5 Campbell, D. J. and Butcher, E. C. 2002. Rapid acquisition of tissue-specific homing phenotypes by CD4(+) T cells activated in cutaneous or mucosal lymphoid tissues. *J. Exp. Med.* 195:135.
6 Yoneyama, H., Matsuno, K., Zhang, Y., Murai, M., Itakura, M., Ishikawa, S., Hasegawa, G., Naito, M., Asakura, H. and Matsushima, K. 2001. Regulation by chemokines of circulating dendritic cell precursors, and the formation of portal tract-associated lymphoid tissue, in a granulomatous liver disease. *J. Exp. Med.* 193:35.
7 Yoneyama, H., Narumi, S., Zhang, Y., Murai, M., Baggiolini, M., Lanzavecchia, A., Ichida, T., Asakura, H. and Matsushima, K. 2002. Pivotal role of dendritic cell-derived CXCL10 in the retention of T helper cell 1 lymphocytes in secondary lymph nodes. *J. Exp. Med.* 195:1257.
8 Ishige, I., Usui, Y., Takemura, T. and Eishi, Y. 1999. Quantitative PCR of mycobacterial and propionibacterial DNA in lymph nodes of Japanese patients with sarcoidosis. *Lancet* 354:120.
9 Fujioka, N., Mukaida, N., Harada, A., Akiyama, M., Kasahara, T., Kuno, K., Ooi, A., Mai, M. and Matsushima, K. 1995. Preparation of specific antibodies against murine IL-1ra and the establishment of IL-1ra as an endogenous regulator of bacteria-induced fulminant hepatitis in mice. *J. Leukoc. Biol.* 58:90.
10 Nagakawa, J., Hishinuma, I., Hirota, K., Miyamoto, K., Yamanaka, T., Tsukidate, K., Katayama, K. and Yamatsu, I. 1990. Involvement of tumor necrosis factor-alpha in the pathogenesis of activated macrophage-mediated hepatitis in mice. *Gastroenterology* 99:758.
11 Yoneyama, H., Harada, A., Imai, T., Baba, M., Yoshie, O., Zhang, Y., Higashi, H., Murai, M., Asakura, H. and Matsushima, K. 1998. Pivotal role of TARC, a CC chemokine, in bacteria-induced fulminant hepatic failure in mice. *J. Clin. Invest.* 102:1933.
12 Cella, M., Jarrossay, D., Facchetti, F., Alebardi, O., Nakajima, H., Lanzavecchia, A. and Colonna, M. 1999. Plasmacytoid monocytes migrate to inflamed lymph nodes and produce large amounts of type I interferon. *Nat. Med.* 5:919.
13 del Hoyo, G. M., Martin, P., Vargas, H. H., Ruiz, S., Arias, C. F. and Ardavin, C. 2002. Characterization of a common precursor population for dendritic cells. *Nature* 415:1043.
14 Scheinecker, C., McHugh, R., Shevach, E. M. and Germain, R. N. 2002. Constitutive presentation of a natural tissue autoantigen exclusively by dendritic cells in the draining lymph node. *J. Exp. Med.* 196:1079.
15 Steinman, R. M. and Nussenzweig, M. C. 2002. Avoiding horror autotoxicus: the importance of dendritic cells in peripheral T cell tolerance. *Proc. Natl Acad. Sci. USA* 99:351.
16 Huang, F. P., Platt, N., Wykes, M., Major, J. R., Powell, T. J., Jenkins, C. D. and MacPherson, G. G. 2000. A discrete subpopulation of dendritic cells transports apoptotic intestinal epithelial cells to T cell areas of mesenteric lymph nodes. *J. Exp. Med.* 191:435.
17 Hancock, W. W., Lu, B., Gao, W., Csizmadia, V., Faia, K., King, J. A., Smiley, S. T., Ling, M., Gerard, N. P. and Gerard, C. 2000. Requirement of the chemokine receptor CXCR3 for acute allograft rejection. *J. Exp. Med.* 192:1515.
18 Tsuji, H., Harada, A., Mukaida, N., Nakanuma, Y., Bluethmann, H., Kaneko, S., Yamakawa, K., Nakamura, S. I., Kobayashi, K. I. and Matsushima, K. 1997. Tumor necrosis factor receptor p55 is essential for intrahepatic granuloma formation and hepatocellular apoptosis in a murine model of bacterium-induced fulminant hepatitis. *Infect. Immun.* 65:1892.
19 Murai, M., Yoneyama, H., Ezaki, T., Suematsu, M., Terashima, Y., Harada, A., Hamada, H., Asakura, H., Ishikawa, H. and Matsushima, K. 2003. Peyer's patch is the essential site in initiating murine acute and lethal graft-versus-host reaction. *Nat. Immunol.* 4:154.
20 Narumi, S., Onozato, M. L., Tojo, A., Sakamoto, S. and Tamatani, T. 2001. Tissue-specific induction of E-selectin in glomeruli is augmented following diabetes mellitus. *Nephron* 89:161.
21 Sasaki, S., Yoneyama, H., Suzuki, K., Suriki, H., Aiba, T., Watanabe, S., Kawauchi, Y., Kawachi, H., Shimizu, F., Matsushima, K., Asakura, H. and Narumi, S. 2002. Blockade of CXCL10 protects mice from acute colitis and enhances crypt cell survival. *Eur. J. Immunol.* 32:3197.

22 Onai, N., Zhang, Y., Yoneyama, H., Kitamura, T., Ishikawa, S. and Matsushima, K. 2000. Impairment of lymphopoiesis and myelopoiesis in mice reconstituted with bone marrow-hematopoietic progenitor cells expressing SDF-1-intrakine. *Blood* 96:2074.
23 Kudo, S., Matsuno, K., Ezaki, T. and Ogawa, M. 1997. A novel migration pathway for rat dendritic cells from the blood: hepatic sinusoids-lymph translocation. *J. Exp. Med.* 185:777.
24 Uwatoku, R., Akaike, K., Yamaguchi, K., Kawasaki, T., Ando, M. and Matsuno, K. 2001. Asialoglycoprotein receptors on rat dendritic cells: possible roles for binding with Kupffer cells and ingesting virus particles. *Arch. Histol. Cytol.* 64:223.
25 Morikawa, S., Baluk, P., Kaidoh, T., Haskell, A., Jain, R. K. and McDonald, D. M. 2002. Abnormalities in pericytes on blood vessels and endothelial sprouts in tumors. *Am. J. Pathol.* 160:985.
26 O'Keeffe, M., Hochrein, H., Vremec, D., Scott, B., Hertzog, P., Tatarczuch, L. and Shortman, K. 2003. Dendritic cell precursor populations of mouse blood: identification of the murine homologues of human blood plasmacytoid pre-DC2 and CD11c+ DC1 precursors. *Blood* 101:1453.
27 Gazitt, Y. 2000. Immunologic profiles of effector cells and peripheral blood stem cells mobilized with different hematopoietic growth factors. *Stem Cells* 18:390.
28 Kunkel, E. J. and Butcher, E. C. 2002. Chemokines and the tissue-specific migration of lymphocytes. *Immunity* 16:1.
29 Mueller, S. N., Jones, C. M., Smith, C. M., Heath, W. R. and Carbone, F. R. 2002. Rapid cytotoxic T lymphocyte activation occurs in the draining lymph nodes after cutaneous herpes simplex virus infection as a result of early antigen presentation and not the presence of virus. *J. Exp. Med.* 195:651.
30 Randolph, G. J., Inaba, K., Robbiani, D. F., Steinman, R. M. and Muller, W. A. 1999. Differentiation of phagocytic monocytes into lymph node dendritic cells *in vivo*. *Immunity* 11:753.
31 Zhao, Y., Chien, S. and Weinbaum, S. 2001. Dynamic contact forces on leukocyte microvilli and their penetration of the endothelial glycocalyx. *Biophys. J.* 80:1124.
32 Lowe, J. B. 2002. Glycosylation in the control of selectin counter-receptor structure and function. *Immunol. Rev.* 186:19.
33 Montoya, M. C., Sancho, D., Vicente-Manzanares, M. and Sanchez-Madrid, F. 2002. Cell adhesion and polarity during immune interactions. *Immunol. Rev.* 186:68.
34 Krug, A., Uppaluri, R., Facchetti, F., Dorner, B. G., Sheehan, K. C., Schreiber, R. D., Cella, M. and Colonna, M. 2002. IFN-producing cells respond to CXCR3 ligands in the presence of CXCL12 and secrete inflammatory chemokines upon activation. *J. Immunol.* 169:6079.
35 Vanbervliet, B., Bendriss-Vermare, N., Massacrier, C., Homey, B., De Bouteiller, O., Briere, F., Trinchieri, G. and Caux, C. 2003. The inducible CXCR3 ligands control plasmacytoid dendritic cell responsiveness to the constitutive chemokine stromal cell-derived factor 1 (SDF-1)/CXCL12. *J. Exp. Med.* 198:823.
36 Swarte, V. V., Joziasse, D. H., Van den Eijnden, D. H., Petryniak, B., Lowe, J. B., Kraal, G. and Mebius, R. E. 1998. Regulation of fucosyltransferase-VII expression in peripheral lymph node high endothelial venules. *Eur. J. Immunol.* 28:3040.
37 Hoke, D., Mebius, R. E., Dybdal, N., Dowbenko, D., Gribling, P., Kyle, C., Baumhueter, S. and Watson, S. R. 1995. Selective modulation of the expression of L-selectin ligands by an immune response. *Curr. Biol.* 5:670.
38 Nakano, H., Yanagita, M. and Gunn, M. D. 2001. CD11c(+)B220(+)Gr-1(+) cells in mouse lymph nodes and spleen display characteristics of plasmacytoid dendritic cells. *J. Exp. Med.* 194:1171.
39 Martin, P., Ruiz, S. R., del Hoyo, G. M., Anjuere, F., Vargas, H. H., Lopez-Bravo, M. and Ardavin, C. 2002. Dramatic increase in lymph node dendritic cell number during infection by the mouse mammary tumor virus occurs by a CD62L-dependent blood-borne DC recruitment. *Blood* 99:1282.
40 Zhang, Y., Yoneyama, H., Wang, Y., Ishikawa, S., Hashimoto, S., Gao, J. L., Murphy, P. and Matsushima, K. 2004. Mobilization of dendritic cell precursors into the circulation by administration of MIP-1alpha in mice. *J. Natl Cancer Inst.* 96:201.
41 Janatpour, M. J., Hudak, S., Sathe, M., Sedgwick, J. D. and McEvoy, L. M. 2001. Tumor necrosis factor-dependent segmental control of MIG expression by high endothelial venules in inflamed lymph nodes regulates monocyte recruitment. *J. Exp. Med.* 194:1375.
42 Jahnsen, F. L., Moloney, E. D., Hogan, T., Upham, J. W., Burke, C. M. and Holt, P. G. 2001. Rapid dendritic cell recruitment to the bronchial mucosa of patients with atopic asthma in response to local allergen challenge. *Thorax* 56:823.
43 Zou, W., Machelon, V., Coulomb-L'Hermin, A., Borvak, J., Nome, F., Isaeva, T., Wei, S., Krzysiek, R., Durand-Gasselin, I., Gordon, A. *et al.* 2001. Stromal-derived factor-1 in human tumors recruits and alters the function of plasmacytoid precursor dendritic cells. *Nat. Med.* 7:1339.
44 Uwatoku, R., Suematsu, M., Ezaki, T., Saiki, T., Tsuiji, M., Irimura, T., Kawada, N., Suganuma, T., Naito, M., Ando, M. and Matsuno, K. 2001. Kupffer cell-mediated recruitment of rat dendritic cells to the liver: roles of *N*-acetylgalactosamine-specific sugar receptors. *Gastroenterology* 121:1460.
45 Martin-Fontecha, A., Sebastiani, S., Hopken, U. E., Uguccioni, M., Lipp, M., Lanzavecchia, A. and Sallusto, F. 2003. Regulation of dendritic cell migration to the draining lymph node: impact on T lymphocyte traffic and priming. *J. Exp. Med.* 198:615.